5500 *Macromolecules* **2010**, *43*, 5500–5502
DOI: 10.1021/ma100915u

Macromolecules
COMMUNICATION TO THE EDITOR

Mechanically Coupled Internal Coordinates of Ionomer Vibrational Modes

Matthew Webber,[†] Nicholas Dimakis,[‡] Dunesh Kumari,[†] Michael Fuccillo,[†] and Eugene S. Smotkin*,[†]

[†]*Department of Chemistry and Chemical Biology, Northeastern University, 360 Huntington Ave, Boston, Massachusetts 02115, and* [‡]*Department of Physics and Geology, University of Texas-Pan American, 1201 W University Dr., Edinburg, Texas 78539*

Received April 26, 2010
Revised Manuscript Received June 1, 2010

Nafion, a sulfonated tetrafluoroethylene copolymer, and its short-side-chain derivative revolutionized low-temperature fuel cell development. Nevertheless, after over 7000 publications on Nafion since 1975,[1] the definitive assignment of key infrared (IR) peaks, including those associated with the SO_3^- exchange group and the ether linkages, has been elusive. Nafion and relevant derivatives are given in Scheme 1.

The highlights of reported interpretations of selected IR spectra (Figure 1a−f) provide the context for this Communication. The attenuated total reflectance (ATR) spectra of hydrated Nafion (a) and the short-side-chain ionomer (b) (i.e., Scheme 1) focus on the ~1060 cm^{-1} and a multiplet that includes a shoulder at 995 cm^{-1} and two peaks ~983 and 970 cm^{-1}, hereafter referred to as $\bar{\nu}_{hf}$ and $\bar{\nu}_{lf}$, respectively. The $\bar{\nu}_{hf}$ and $\bar{\nu}_{lf}$ have been conventionally assigned to ether groups in proximity to the backbone and the sulfonate group, respectively. Cable et al.[2] associated $\bar{\nu}_{lf}$ to the ether linkage closest to the sulfonate group because of its enhanced sensitivity to ion exchange and the fact that the $\bar{\nu}_{lf}$ persists in the Dow short-side-chain ionomer spectrum. The short-side-chain ionomer has only one ether group, positioned adjacent to the sulfonate group. The sulfonyl fluoride precursor was also compared to Nafion. In the sulfonyl fluoride spectrum (c), $\bar{\nu}_{lf}$ diminishes concurrently with the ~1060 cm^{-1} peak. These observations were reconciled by invoking solvation effects as responsible for the sensitivity of $\bar{\nu}_{lf}$ to ion exchange because in hydrated Nafion, the sulfonate group is embedded in an aqueous phase. Therefore, the ether group in closest proximity to the sulfonate group may be subject to solvation as well and thus sensitive to ion exchange. The $\bar{\nu}_{hf}$, which is essentially insensitive to ion exchange, has been attributed to the ether link distant from the sulfonate group. Further, Cable[2] concluded that the concurrent loss of the 1060 cm^{-1} peak is due to the loss of the SO_3^- symmetric mode.

The association of the 1060 cm^{-1} peak and $\bar{\nu}_{lf}$, solely with SO_3^- and ether link modes, respectively, precludes proper analysis of the spectra. However, if the mechanical coupling of the internal coordinates of the SO_3^- and its near-neighbor COC are considered, the analysis of 1060 cm^{-1} and $\bar{\nu}_{lf}$ peaks of Figure 1 can be reconciled without the need for invoking solvation of the ether link (vide infra). Warren and McQuillan[3] noted the importance of the considering vibrational contributions from more than one functional group when assigning IR absorptions of fluoropolymers. Byun et al.[4] also reported the same loss of the $\bar{\nu}_{lf}$ upon substitution of the sulfonic acid group for a sulfonyl imide (spectrum f) and assigned $\bar{\nu}_{lf}$ as did Cable et al. (Figure 1e,f).

*To whom correspondence should be addressed.

Scheme 1. Structures of Nafion and Derivatives

R: -SO_3H (Nafion)
-SO_2F (sulfonyl fluoride)
-$SO_2N(H)SO_2CF_3$ (-sulfonyl imide)

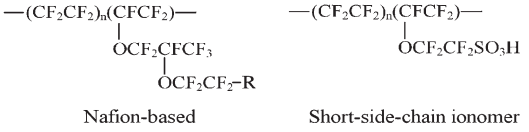

Nafion-based Short-side-chain ionomer

Transmission infrared spectra of Nafion 112 were obtained on a Bruker Vertex 80V spectrometer (Bruker Optics Inc., Billerica, MA) under dry air or vacuum. All spectra were an average of 100 scans. The Nafion samples were dehydrated on a vacuum line at 10^{-2} Torr (under nitrogen) at 135 °C for several hours. Samples were transferred to a drybox for sample holder installation in order to minimize atmospheric exposure. The transmission spectra (Figure 2) show a concurrent loss of intensity of 1062 cm^{-1} and $\bar{\nu}_{lf}$ due to dehydration of the membrane, simultaneous with evolution of peaks at 1415 and 908 cm^{-1}.

We attribute the transition of the dehydrated (red) to the hydrated (blue) spectrum to a change in the point group symmetry of the sulfonic acid group (vide infra). The following density functional theory (DFT) calculations show that as the proton dissociates from the sulfonic acid group (e.g., with hydration), the local point group symmetry changes from C_1 to C_{3v}.

Unrestricted DFT[5,6] with the hybrid X3LYP[7] functional was used for geometry optimization and calculations of the normal-mode frequencies and corresponding IR spectra of triflic acid, the Nafion side chain (NSC), and the NSC with a PTFE backbone segment (NSCB). The calculations were done at water/sulfonate ratios (λ)[8] from 0 to 10. The X3LYP extension of the B3LYP[9] functional yields more accurate heats of formation. The all-electron 6-311G**++ Pople triple-ζ basis set is used in all calculations ("**" and "++" denote polarization[10] and diffuse[11] basis set functions, respectively). Jaguar 6.5 (Schrodinger Inc., Portland, OR) uses the pseudospectral method[12] for calculation of time-consuming integrals with the same accuracy as the fully analytical DFT codes.

Images of the geometry optimized NSC and NSCB anion are shown in Figure 3.

Figure 4 shows DFT optimized structures of the triflic acid exchange site as water molecules are sequentially added. The option to include a dielectric in the calculation was not used because the effect of such an option would be a small perturbation over the effects due to sequential addition of water molecules to the solvation sphere. The triflic acid calculations reveal a threshold λ (λ_d) where the SO−H bond dissociates (Figure 4, top right), and a $\lambda_{i\text{-}o}$, where the H_3O^+ loses a direct hydrogen bond to the sulfonic acid anion (Figure 4, bottom right.) Paddison used B3LYP/6-31G** to calculate λ_d and $\lambda_{i\text{-}o}$ of 3 and 6, respectively.[13] Although different from our values of 4 and 10, respectively, the near-identical O−H and O−O distances support the converged energies of both Paddison and our calculations (see Table 1).

Our higher value of λ_d results from the use of diffuse basis set functions. Spitznagel et al.[14] observed significant changes to optimized geometries involving anions and proton affinity when using diffuse functions. To confirm the findings of Spitznagel,[14] the triflic acid structure was optimized for $\lambda = 3$ without diffuse functions, resulting in the same λ_d as Paddison. This provides confidence in our attribution to diffuse functions for a higher

 Published on Web 06/08/2010

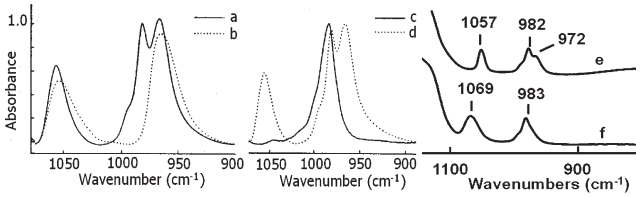

Figure 1. (a) Nafion-H, (b) short-side-chain ionomer, (c) sulfonyl fluoride, (d) Nafion-H, (e) H^+ form of Nafion, and (f) sulfonyl imide. Spectra a−d adapted from Cable et al.[2] Spectra e and f adapted from ref 4.

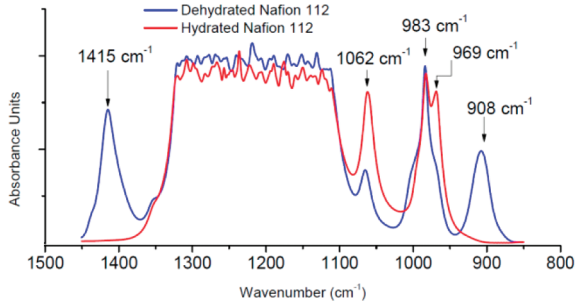

Figure 2. Transmission IR spectra of Nafion 112 showing the evolution of 1415 and 908 cm^{-1} bands upon dehydration.

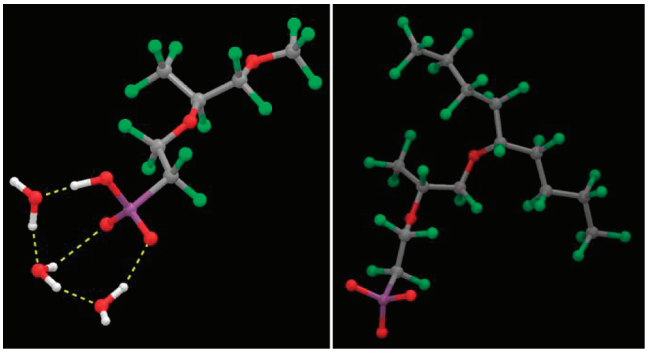

Figure 3. NSC $\lambda = 3$ (left); NSCB anion (right) (red = O, white = H, gray = C, purple = S, green = F, yellow dotted lines = H-bonds).

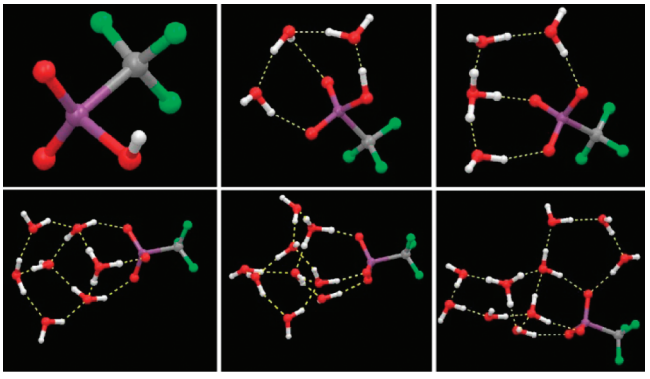

Figure 4. Proton dissociation threshold and the formation of H_3O^+ and C_{3v} local symmetry. Top: $\lambda = 0$, left; $\lambda = 3$, center; $\lambda = 4$, right. Bottom: $\lambda = 7$, left; $\lambda = 9$, center; $\lambda = 10$, right (red = O, white = H, gray = C, purple = S, green = F, yellow dotted lines = H-bonds).

value of λ_d. We attribute our higher value of $\lambda_{i\text{-}o}$ to the use of X3LYP, developed to significantly improve hydrogen bonding and van der Waals interactions over B3LYP.[7] A comparison to similar computational studies of trilfic acid λ_d and $\lambda_{i\text{-}o}$ values is summarized in the Supporting Information.[13,15−18]

Table 1. Comparison of the Acidic Proton O−H Distances and the O−O Distances about the Central Hydrogen Ion for Triflic Acid

	SO−H (Å)		SO−H−OH (Å)	
λ	Paddison[13]	present	Paddison[13]	present
0	0.973	0.970		
1	1.02	1.004	2.595	2.628
2	1.059	1.037	2.496	2.531
3	1.562	1.074	2.556	2.465
4	1.721	1.522	2.658	2.526
5	1.739	1.481	2.693	2.503
6	3.679	1.49	4.243	2.519
7		1.511		2.523
8		1.528		2.539
9		1.523		2.539
10		3.677		4.372

Table 2. Comparison of O−H Distance for the Acidic Proton and the O−O Distance to the Central Hydronium O (or Nearest Water Molecule)

	SO−H (Å)		SO−H−OH (Å)	
λ	triflic acid	NSC	triflic acid	NSC
3	1.074	1.077	2.465	2.464
4	1.522	1.531	2.526	2.541
7	1.511	1.526	2.523	2.533
9	1.523	1.532	2.539	2.545

Extension of the λ-dependent calculations to NSC confirms a $\lambda_d = 4$, consistent with the triflic acid calculations. NSC calculations at $\lambda = 7$ and 9 confirm a $\lambda_{i\text{-}o}$ greater than 9. The SO−H and SO−H−OH distances versus λ are presented in Table 2. The similarities between the O−H and O−O distances of solvated triflic acid and NSC, versus λ, suggests that at the levels of hydration calculated the sulfonic acid group behavior is rather generic.

Although hydrated Nafion has C_1 symmetry overall, it has regions of local symmetry, namely the $-SO_3^-$ (C_{3v}) and the ether groups (C_{2v}). Maestro (Schrodinger Inc., Portland, OR) converts Jaguar output files to vibrational mode animations. The full animations of selected calculated modes are in the Supporting Information. Snapshots of the $CF_3SO_3^-$ symmetric stretch ($\nu_s(A_1)$) and the CF_3OCF_3 asymmetric ($\nu_{as}(B_2)$) and rocking modes ($\rho_r(B_2)$) and associated frequencies are shown (Figure 5, top row).

Hereafter, the $\nu_s(A_1)$, $\nu_{as}(B_2)$, and $\rho_r(B_2)$ modes are referred to as "pure modes". The equilibrium positions and vibrational mode extrema of NSCB modes corresponding to the bands at 969 cm^{-1} ($\bar{\nu}_{lf}$) and 1060 cm^{-1} (Figure 2) are shown in Figure 5. The animations enable visualization of how the pure mode internal coordinates mechanically couple to yield the NSCB modes. The center row snapshots show a 983 cm^{-1} NSCB mode[20] that results from the coupling of the $\nu_s(A_1)$, $\nu_{as}(B_2)$, and $\rho_r(B_2)$ with the dominate mode being the $\nu_s(A_1)$. The full animations show that the dominate pure mode of the 1060 cm^{-1} peak is actually the CF_3OCF_3 $\nu_{(as)}(B_2)$ mode with a much weaker contribution from the $\nu_s(A_1)$ of triflic acid. The 1060 cm^{-1} is primarily a $\nu_{as}(B_2)$ mode mechanically coupled to the internal coordinates of the $\nu_s(A_1)$ of the SO_3^- group. The key point is that the ether link nearest the exchange group has internal coordinates that are mechanically coupled to the $\nu_s(A_1)$ mode: The 1060 cm^{-1} and $\bar{\nu}_{lf}$ peaks cannot be purely ascribed to the SO_3^- and COC modes, respectively.

In fact, ν_{lf}, conventionally assigned as an ether mode, derives from the triflic acid SO_3^- $\nu_s(A_1)$ mode with a calculated average of 974 cm^{-1} (see Table 3).

The above analysis obviates the need to invoke ether link solvation for analysis of the Figure 1 spectra. Because the internal coordinates of the 1060 cm^{-1} and ν_{lf} peaks are mechanically

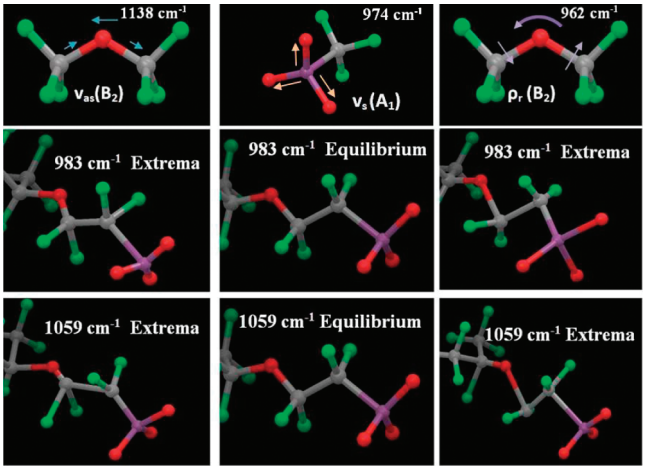

Figure 5. Maestro animation snapshots of DFT calculated modes of the full side chain and backbone: (top row) small molecule "pure" modes; (middle row) 983 cm^{-1}, equilibrium positions in center panel; (bottom row) 1060 cm^{-1}, equilibrium positions in center panel. Extrema at left and right panels of center panels. AVI animations are given in the Supporting Information.

Table 3. Calculated $\nu_s(A_1)$ Mode of C_{3v} (i.e., λ_d or Greater) Sulfonate

	triflic acid SO_3^- sym str (cm^{-1})		triflic acid SO_3^- sym str (cm^{-1})
$\lambda = 4$	978	$\lambda = 8$	979
$\lambda = 5$	965	$\lambda = 9$	980
$\lambda = 6$	980	$\lambda = 10$	975
$\lambda = 7$	964		

coupled, *they always shift* (*upon ion exchange of the SO_3^- group*) *or diminish together* (*upon dehydration,* Figure 2).

Reconsider the spectra of Figure 1 in light of mechanically coupled internal coordinates. The $\bar{\nu}_{hf}$ is not in the short-side-chain spectra (b) because $\bar{\nu}_{hf}$ was the backbone ether link that was not mechanically coupled to the SO_3^-. In the short-side-chain derivative, the remaining $\bar{\nu}_{lf}$ is now the backbone ether link mechanically coupled to the SO_3^- group (i.e., the functional groups responsible for the mechanically coupled $\nu_s(A_1)$, $\nu_{as}(B_2)$, and $\rho_r(B_2)$ are now in close proximity to the backbone). In the sulfonyl fluoride spectra (c), the C_{3v} symmetry of the SO_3^- is lost.

Thus, similar to the case of dehydration (Figure 2), the $\bar{\nu}_{lf}$ and 1060 cm^{-1} peaks vanish. The sulfonyl imide spectra (f) behaves similarly to that of the sulfonyl fluoride. The remaining peak at 1069 cm^{-1} is not inconsistent with our analysis. Korzeniewski confirmed this peak as the asymmetric S−N−S stretch.

Warren and McQuillan[3] recognized that Nafion vibrational modes have contributions from multiple functional groups using DFT at the B3LYP/6-311G+(d,p) level of theory. Their calculated 929 cm^{-1} mode was assigned to a coupling of C−S stretching and SO_3^- symmetric stretching to explain the loss of the 971 cm^{-1} band upon dehydration. Okamoto[19] calculated peaks at 989 and 1060 cm^{-1} as SO_3^- symmetric and COC (nearest the headgroup) asymmetric stretching, respectively, for a model side chain of Nafion in its anion form, $(CF_3)_2CFOCF_2CF(CF_3)$-$OCF_2CF_2SO_3^-$, using B3LYP/6-31G(d,p)++.

The 1060 cm^{-1} and $\bar{\nu}_{lf}$ peaks result from the mechanical coupling of the internal coordinates of SO_3^- and the COC "pure" modes. The 1060 cm^{-1} mode is dominated by an ether link mode. The calculated mode at 983 cm^{-1}, a major contributor to the $\bar{\nu}_{lf}$ peak, is dominated by the SO_3^- $\nu_s(A_1)$ mode. The consideration of mechanically coupled internal coordinates is essential for the analysis of infrared spectra of ionomers and correlation of those spectra with the effects of ion exchange and state of hydration.

Acknowledgment. We thank the UT Pan American High Performance Computing Center and comments from reviewer #1 and Max Diem. Funding was provided by ARO DURIP W911NF-07-1-0236.

Supporting Information Available: Maestro animations and summary table of proton dissociation studies. This material is available free of charge via the Internet at http://pubs.acs.org.

References and Notes

(1) ISI Web of Knowledge Home Page, **2009**; Vol. *2009*.
(2) Cable, K. M.; Mauritz, K. A.; Moore, R. B. *J. Polym. Sci., Part B: Polym. Phys.* **1995**, *33*, 1065.
(3) Warren, D. S.; McQuillan, A. J. *J. Phys. Chem. B* **2008**, *112*, 10535.
(4) Byun, C. K.; Sharif, I.; DesMarteau, D. D.; Creager, S. E.; Korzeniewski, C. *J. Phys. Chem. B* **2009**, *113*, 6299.
(5) Hohenberg, P.; Kohn, W. *Phys. Rev. B* **1964**, *136*, 864.
(6) Kohn, W.; Sham, L. J. *Phys. Rev. A* **1965**, *140*, 1133.
(7) Xu, X.; Zhang, Q. S.; Muller, R. P.; Goddard, W. A. *J. Chem. Phys.* **2005**, *122*, 14.
(8) Zawodzinski, T. A., Jr.; Derouin, C.; Radzinski, S.; Sherman, R. J.; Smith, V. T.; Springer, T. E.; Gottesfeld, S. *J. Electrochem. Soc.* **1993**, *140*, 1041.
(9) Becke, A. D. *J. Chem. Phys.* **1993**, *98*, 5648.
(10) Frisch, M. J.; Pople, J. A.; Binkley, J. S. *J. Chem. Phys.* **1984**, *80*, 3265.
(11) Clark, T.; Chandrasekhar, J.; Spitznagel, G. W.; Schleyer, P. V. R. *J. Comput. Chem.* **1983**, *4*, 294.
(12) Langlois, J. M.; Muller, P. R.; Coley, T. R.; Goddard, W. A.; Ringnalda, M. N.; Won, Y. F. R. *J. Chem. Phys.* **1990**, *92*, 7488.
(13) Paddison, S. J. *J. New Mater. Electrochem. Syst.* **2001**, *4*, 197.
(14) Spitznagel, G.; Timothy, C.; Paul von Ragué, S.; Warren, J. H. *J. Comput. Chem.* **1987**, *8*, 1109.
(15) Glezakou, V. A.; Dupuis, M.; Mundy, C. J. *Phys. Chem. Chem. Phys.* **2007**, *9*, 5752–5760.
(16) Li, X. B.; Liao, S. J. *J. Mol. Struct.: THEOCHEM* **2009**, *897* (1−3), 66–68.
(17) Sagarik, K.; Phonyiem, M.; Lao-Ngam, C.; Chaiwongwattana, S. *Phys. Chem. Chem. Phys.* **2008**, *10*, 2098–2112.
(18) Koyama, M.; Bada, K.; Sasaki, K.; Tsuboi, H.; Endou, A.; Kubo, M.; Del Carpio, C. A.; Broclawik, E.; Miyamoto, A. *J. Phys. Chem. B* **2006**, *110*, 17872–17877.
(19) Okamoto, Y. *Chem. Phys. Lett.* **2004**, *389*, 64.
(20) This calculated value corresponds to the experimental 969 cm^{-1}, not to be confused with the experimental 983 cm^{-1} .